Active and Thermal Fluctuations in Multi-scale Polymer Structure and Dynamics: Supplemental materials

Ashesh Ghosh[1] and Andrew J. Spakowitz[1,2,3,†]
1. Department of Chemical Engineering, Stanford University, Stanford, CA 94305
2. Biophysics Program, Stanford University, Stanford, CA 94305
3. Department of Materials Science & Engineering, Stanford University, Stanford, CA 94305

I. ALGORITHM TO GENERATE ACTIVE-BROWNIAN POLYMER CONFORMATIONS

The conformation of an active-Brownian polymer is selected from the appropriate steady-state distribution that captures the correlated active forces at all times prior to the initial time (i.e. all times from $-\infty$ to $\tau_0 = 0$). This distribution captures both the statistics of the active forces (Gaussian distributed with temporal correlation) and the normal-mode amplitude. Our work [1] provides the necessary input to determine the normal-mode statistics and generate the normal-mode amplitudes that define the chain conformation of an active-Brownian polymer. To aid in the use of this algorithm, we transform our normal-mode treatment, which depends on the mode index p, to a form that is consistent with a particle in a harmonic trap that is independent of p. We define the dimensionless variables

$$u = \frac{p}{\sqrt{N}}\frac{\sqrt{3\pi^2}}{b}X_p^{(x)} \tag{S1}$$

$$\tilde{F}^{(B)} = \frac{\sqrt{N}}{p}\frac{b}{\sqrt{3\pi^2}k_BT}f_p^{(B,x)} \tag{S2}$$

$$\tilde{F}^{(A)} = \frac{\sqrt{N}}{p}\frac{b}{\sqrt{3\pi^2}k_BT}f_p^{(A,x)} \tag{S3}$$

$$\tilde{F}_A^2 = \frac{\Gamma N^2 K_A}{p^2} \tag{S4}$$

$$\tilde{K}_A = \frac{N^2 K_A}{p^2} \tag{S5}$$

$$\tilde{\tau} = \frac{p^2\tau}{N^2} \tag{S6}$$

where $X_p^{(x)} = \hat{\delta}_x \cdot \vec{X}_p$ is the x-component of the normal-amplitude vector (similar definition for $f_p^{(B,x)}$ and $f_p^{(A,x)}$). This allows us to write the governing Langevin equation in the p-independent form

$$\frac{\partial u}{\partial \tilde{\tau}} = -u + \tilde{F}^{(B)} + \tilde{F}^{(A)} \tag{S7}$$

where

$$\langle \tilde{F}^{(B)}(\tilde{\tau})\tilde{F}^{(B)}(\tilde{\tau}')\rangle = 2\delta(\tilde{\tau}-\tilde{\tau}') \tag{S8}$$

$$\langle \tilde{F}^{(A)}(\tilde{\tau})\tilde{F}^{(A)}(\tilde{\tau}')\rangle = \tilde{F}_A^2 \exp\Big(-\tilde{K}_A|\tilde{\tau}-\tilde{\tau}'|\Big) \tag{S9}$$

From our work [1] the initial distribution for the p-independent normal-mode amplitude u_0 and p-independent active force $\tilde{F}_A^{(0)}$ is given by

$$\mathcal{P}_0(u_0,\tilde{F}_A^{(0)}) = \frac{1}{\mathcal{N}}\exp\left\{-\frac{[u_0-\tilde{F}_A^{(0)}/(1+\tilde{K}_A)]^2}{2[1+\tilde{F}_A^2\tilde{K}_A/(1+\tilde{K}_A)^2]} - \frac{(\tilde{F}_A^{(0)})^2}{2\tilde{F}_A^2}\right\} \tag{S10}$$

The normalization constant $\mathcal{N}$ is found to be $\mathcal{N} = 2\pi\tilde{F}_A[1+\tilde{F}_A^2K_A/(1+K_A)^2]^{1/2}$. The y- and z-components are governed by the same equations, are separable from each other, and are thus independently and identically distributed.

This distribution is used to generate the p-independent normal-mode amplitude u_0 and p-independent active force $\tilde{F}_A^{(0)}$ for each spatial direction x, y, and z and each normal mode. We then convert these back to the p-dependent

normal modes $\vec{X}_p$ and active forces $\vec{f}_p^{(A)}$ using the expressions in Eq. S1-S6, and use Eq. 6 of our manuscript to generate the active-Brownian polymer conformations that appear in Figs. 1 and 2 of our manuscript.

II. EFFECTIVE COARSE-GRAINED GAUSSIAN FORCE MODEL

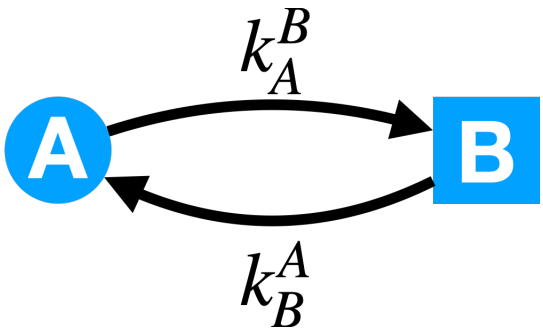

FIG. S1: Effective coarse grained two-state model. In state A and B the system experiences a random force of $\vec{f}_A$ and $\vec{f}_B$ respectively. The rate of switch from state $\alpha \in \{A, B\}$ to $\beta \in \{B, A\}$ is given as k_α^β.

We justify the use of our effective coarse-grained Gaussian force model. We consider a stochastic active force with a fixed magnitude $\vec{f}_A$ in A-state. Due to chemical processes the state of the system switches back and forth between states A and B as a telegraph noise process as schematically shown in Fig. S1. In state B, the force experienced is $\vec{f}_B$. We consider the system to be following a telegraphic noise statistics with switch rates of

$$\begin{aligned} k_{A\to B} &\equiv k_A^B \\ k_{B\to A} &\equiv k_B^A \end{aligned} \tag{S11}$$

Our goal is to understand the effective force experienced due to M-uncorrelated telegraphic noise process. In steady state, the probability of A and B states are given purely as a function of individual switching rates by,

$$\begin{aligned} p_A &= \frac{k_B^A}{k_A^B + k_B^A} \\ p_B &= \frac{k_A^B}{k_A^B + k_B^A} \end{aligned} \tag{S12}$$

. We can define a probability density for force in α-state as,

$$p_f(\alpha) = \frac{1}{4\pi|\vec{f}|^2}\delta(|\vec{f}| - f_\alpha) \tag{S13}$$

We can write the Green's function for forces by looking at path summations over chemical states A and B. Hence the joint probability of starting at state α (at time $t = 0$) and ending at α (at time $t = t > 0$) is,

$$\mathcal{P}_\alpha[\vec{f}|\vec{f}_0; t] = \delta(\vec{f} - \vec{f}_0) f_\alpha(\vec{f}_0) \exp\left(-k_\alpha^\beta t\right) p_\alpha \tag{S14}$$

where $\beta \neq \alpha$ and if $\alpha \in (A, B)$ then $\beta \in (B, A)$. Similarly, we can consider paths that start at A (or B) and end at B (or A). The Green's function is given as

$$\mathcal{P}_{\alpha\beta}[\vec{f}|\vec{f}_0; t] = \int_0^t dt_1 f_\beta(\vec{f}) \exp[-k_\beta^\alpha (t - t_1)] k_\alpha^\beta f_\alpha(\vec{f}_0) \exp\left(-k_\alpha^\beta t\right) p_\alpha. \tag{S15}$$

This single-path Green's function can be extended to arbitrary chemical-state paths.

To simplify our analysis, we look at the Green's function in Laplace space from t to s and find

$$\begin{aligned}\tilde{\mathcal{P}}_A[\vec{f}|\vec{f}_0;s] &= \delta(\vec{f}-\vec{f}_0)f_A(\vec{f}_0)p_A\frac{1}{s+k_A^B}\\ \tilde{\mathcal{P}}_{AB}[\vec{f}|\vec{f}_0;s] &= f_B(\vec{f})f_A(\vec{f}_0)p_A\frac{1}{s+k_B^A}\frac{k_A^B}{s+k_A^B}\\ \tilde{\mathcal{P}}_{ABA}[\vec{f}|\vec{f}_0;s] &= f_A(\vec{f})f_A(\vec{f}_0)p_A\frac{1}{s+k_A^B}\frac{k_B^A}{s+k_B^A}\frac{k_A^B}{s+k_A^B}\end{aligned} \tag{S16}$$

For the first three chemical-state paths that begin in state A. The sum over all A trajectories that start and end at A is given by

$$\tilde{\mathcal{P}}_{A\to A}(s) = \tilde{\mathcal{P}}_A + \tilde{\mathcal{P}}_{ABA} + \tilde{\mathcal{P}}_{ABABA} + \ldots = \frac{\delta(\vec{f}-\vec{f}_0)f_A(\vec{f}_0)p_A}{s+k_A^B} + \frac{f_B(\vec{f})f_A(\vec{f}_0)p_A}{s+k_A^B}\sum_{n=1}^{\infty}\Big(\frac{k_B^A}{s+k_B^A}\Big)^n\Big(\frac{k_A^B}{s+k_A^B}\Big)^n \tag{S17}$$

Similarly we can find the following expressions,

$$\begin{aligned}\tilde{\mathcal{P}}_{A\to A}(s) &= \frac{\delta(\vec{f}-\vec{f}_0)f_A(\vec{f}_0)p_A}{s+k_A^B} + \frac{f_A(\vec{f})f_A(\vec{f}_0)p_A}{s(s+k_A^B(s+k_A^B+k_B^A)}\\ \tilde{\mathcal{P}}_{B\to B}(s) &= \frac{\delta(\vec{f}-\vec{f}_0)f_B(\vec{f}_0)p_B}{s+k_B^A} + \frac{f_B(\vec{f})f_B(\vec{f}_0)p_B}{s(s+k_B^A(s+k_B^A+k_A^B)}\\ \tilde{\mathcal{P}}_{A\to B}(s) &= \frac{f_B(\vec{f})f_A(\vec{f}_0)p_Ak_A^B}{s(s+k_B^A+k_A^B)}\\ \tilde{\mathcal{P}}_{B\to A}(s) &= \frac{f_A(\vec{f})f_B(\vec{f}_0)p_Bk_B^A}{s(s+k_B^A+k_A^B)}\end{aligned} \tag{S18}$$

We can now look at the governing force distribution of M uncorrelated telegraphic noise forces, where the total force on any state A or B is

$$\vec{F} = \sum_{i=1}^{M}\vec{f}_i \tag{S19}$$

The governing Green's function for the total force is given by

$$\mathcal{P}[\vec{F}|\vec{F}_0;t] = \int\prod_{i=1}^{M}d\vec{f}_i d\vec{f}_{0_i}\prod_{i=1}^{M}p[\vec{f}_i|\vec{f}_{0_i};t]\delta\Big(\vec{F}-\sum_{i=1}^{M}\vec{f}_i\Big)\delta\Big(\vec{F}_0-\sum_{i=1}^{M}\vec{f}_{0_i}\Big) \tag{S20}$$

In Fourier space ($\vec{F}\to\vec{k}$ and $\vec{F}_0\to\vec{k}_0$), the total-force Green's function is written as

$$\hat{\mathcal{P}}[\vec{k}|\vec{k}_0;t] = \prod_{i=1}^{M}\hat{\mathcal{P}}[\vec{k}|\vec{k}_0;t] = \Big[\int d\vec{f}d\vec{f}_0\exp\Big(i\vec{k}\cdot\vec{f}\Big)p[\vec{f}|\vec{f}_0;t]\exp\Big(i\vec{k}_0\cdot\vec{f}_0\Big)\Big]^M \tag{S21}$$

In the large-M limit, we express the total-force Green's function as

$$\hat{\mathcal{P}}[\vec{k}|\vec{k}_0;t] = \mathcal{N}^{-1}\exp\Big[-\frac{M}{6}(k^2+k_0^2)(f_A^2p_A+f_B^2p_B) - \frac{M}{3}\vec{k}\cdot\vec{k}_0\big(f_A^2p_Ae^{-k_A^Bt}+f_B^2p_Be^{-k_B^At}\big)\Big] \tag{S22}$$

Thus, the effective force from a sum of telegraph active forces follows a time-correlated Gaussian distribution, which is consistent with the model used in our work. This analysis can be extended to an arbitrary active-force model governing the individual force processes, provided the moments of the governing distribution are finite.

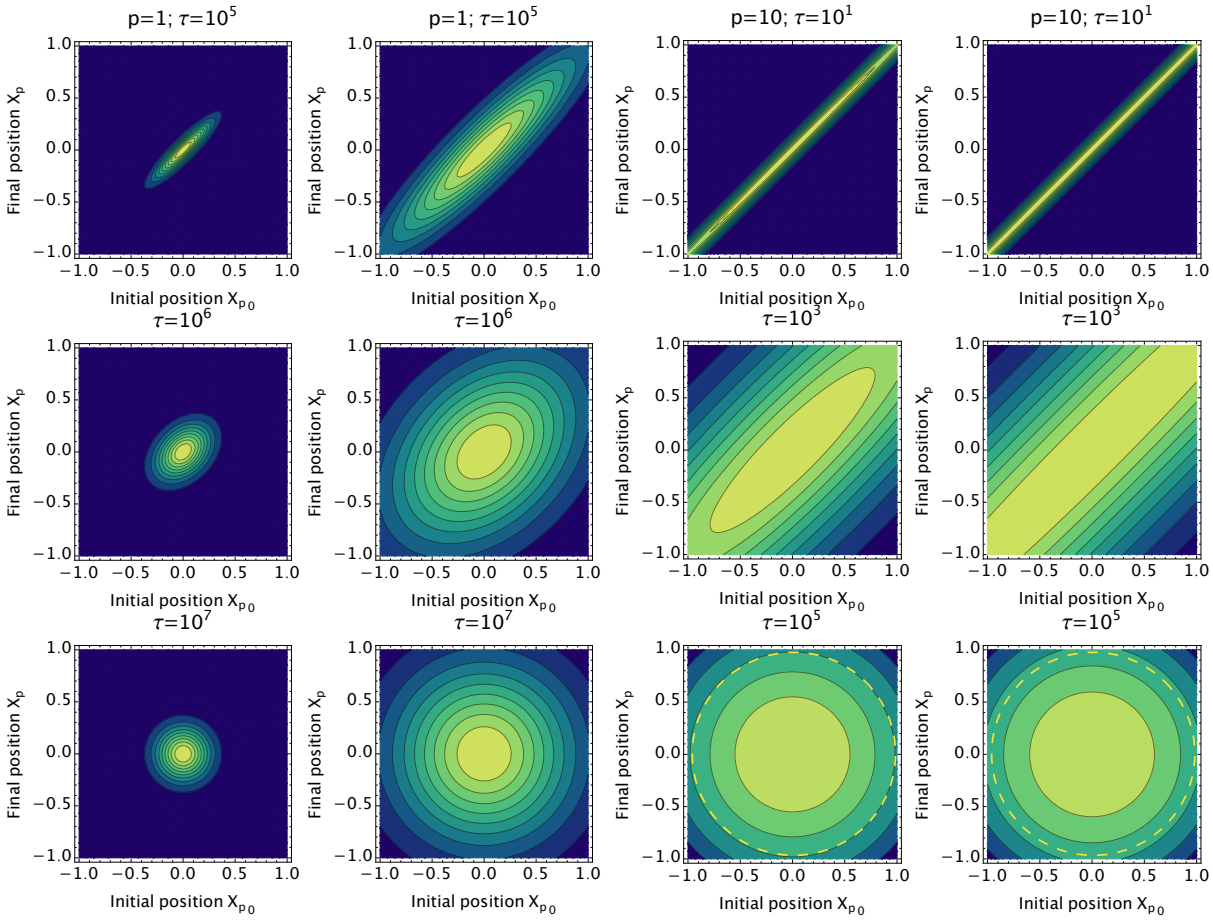

FIG. S2: Two point distributions for individual modes $P_2(\vec{X}_p|\vec{X}_{p_0};\tau)$ are plotted for both Rouse (column 1 and 3) and active Rouse polymer (column 2 and 4) for two different mode numbers of $p = 1$ (col. 1 & 2) and $p = 10$ (col. 3 & 4).

III. MODE AMPLITUDES

To understand length-scale dependent changes we look at the two-point distribution function of individual modes of the Rouse and active Rouse chain respectively with a focus on $p = 1$ (lengthscales of the chain) and $p = 10$ (lengthscales much smaller than the chain). We note that for both the modes, with increasing time the distribution becomes symmetric as correlations are lost. However, for $p = 1$ we can easily note the spread of the distribution of initial (short-time) and final (long-time) distributions is much larger for active Rouse polymer that indicates the large lengthscale swelling of the chain. For $p = 10$, as we concentrate on much smaller lengthscales as compared to the entire chain, at long enough times we note similar probability distributions and only a weak swelling at small lengthscales (yellow dashed line in the two bottom right plots for $P_2 = 0.8$). This illustrates lengthscale dependent swelling of the polymer in terms of the normal modes of the system and complimentary to the analysis of MSCD provided in the main article.

IV. MEAN-SQUARE DISPLACEMENT (MSD)

The mean-square displacement of a segment of the polymer chain, defined as $\mathrm{MSD}(\tau) = \langle(\vec{r}(n,\tau) - \vec{r}(n,0))^2\rangle$ with respect to midpoint of the chain, *i.e.* $n = N/2$ is given by,

$$\mathrm{MSD}(\tau) = \mathrm{MSD}_{\mathrm{com}}(\tau) + 2\sum_{p=1}^{\infty}\mathrm{MSD}_{2p}(\tau) \tag{S23}$$

where, the center of mass MSD is found to be,

$$\mathrm{MSD}_{\mathrm{com}}(\tau) = \langle(\vec{X}_0(\tau) - \vec{X}_0(0))^2\rangle = \frac{6Nk_BT}{k_b}\Big[\Big(\frac{1+\Gamma}{N^2}\Big)\tau + \frac{\Gamma}{N^2K_A}\Big(e^{-K_A\tau} - 1\Big)\Big] \tag{S24}$$

For any generic mode, $p \geq 1$, we find,

$$\mathrm{MSD}_p(\tau) = \langle(\vec{X}_p(\tau) - \vec{X}_p(0))^2\rangle = \frac{6k_BT}{k_p}\Big\{\Big(1 - e^{-\frac{p^2\tau}{N^2}}\Big) + \frac{\Gamma N^2K_A}{N^4K_A^2 - p^4}\Big[N^2K_A\Big(1 - e^{-\frac{p^2\tau}{N^2}}\Big) - p^2\Big(1 - e^{-K_A\tau}\Big)\Big]\Big\} \tag{S25}$$

where, it can be easily identified that, $\mathrm{MSD}_p(\tau) = 2(C_p(0) - C_p(\tau)) = 2\triangle C_p(\tau)$.

Figure S3 plots mean-square displacement (MSD) of the midpoint of the chain as a function of time for the parameters indicated in the caption. Center-of-mass MSD is shown in the right in presence of active forces (orange) with individual thermal (green) and athermal (or, active in blue dashed) contributions.

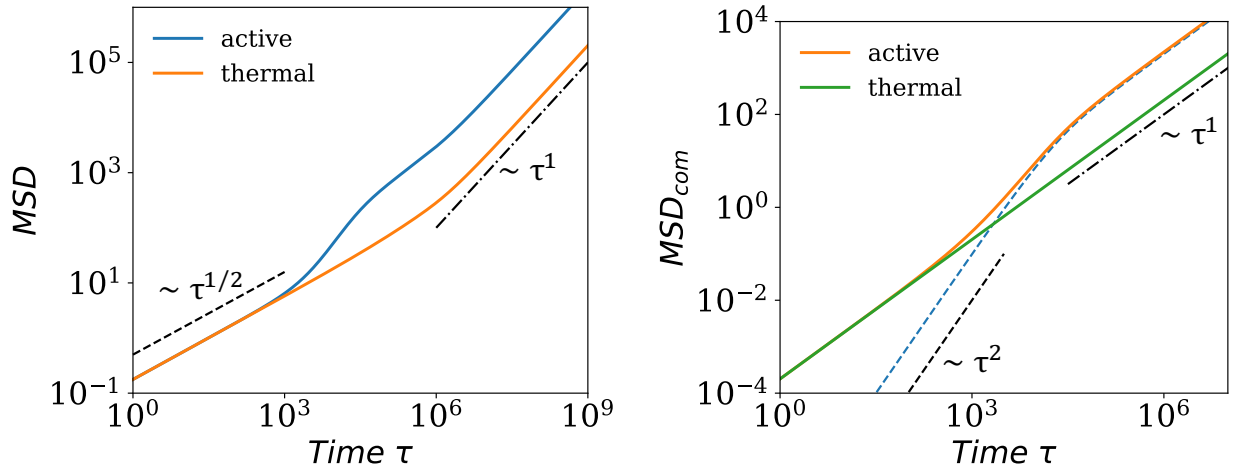

FIG. S3: Center-of-mass (com) mean-squared-displacement (MSD) for a chain length of $N = 1000$ is shown in the right with both thermal and active Rouse model for $\Gamma = 10$ and $K_A = 10^{-4}$. Total chain MSD as a function of time for the same system parameters are shown in left.

Short-time limit: For short times, the COM mean-square displacement has the asymptotic behavior, $\lim_{\tau\to 0}\mathrm{MSD}_{\mathrm{com}}(\tau) \to \frac{6k_BT}{Nk_b}\tau$ that coincides with the center-of-mass mean-square displacement for the Rouse polymer [2]. Hence, at short times the translational motion of the whole chain is not affected by presence of active forces. In the same short time limit we also note the individual modes contribute as, $\lim_{\tau\to 0}\mathrm{MSD}_p(\tau) \to \frac{6k_BT}{Nk_b}\tau$, *i.e.* a mode-index and active force independent contribution. Hence during timescales much shorter than the active force correlation time, not only the center-of mass motion but the entire polymer behaves as a purely thermal fluctuation driven Rouse chain, completely oblivious of active forces in the system. Hence we can expect in biological systems, athermal fluctuations (ATP or enzymatic activity generating biological fluctuations) play ∼no role in determining short time dynamics.

Long-time limit: For the long time limit, we note the asymptotic behavior, $\lim_{\tau\to\infty}\mathrm{MSD}_{\mathrm{com}}(\tau) \to \frac{6k_BT}{Nk_b}(1+\Gamma)\tau$, that reveals an activity dependent effective temperature of the system, defined as, $T^{\mathrm{eff}}_{AB} = T(1+\Gamma)$. The individual modes contribute in the long time limit as, $\lim_{\tau\to\infty}\mathrm{MSD}_p(\tau) \to \frac{6k_BT}{k_p}\Big\{1 + \frac{\Gamma N^2K_A}{N^2K_A + p^2}\Big\}$, a time-independent but mode-index dependent constant factor. Hence at long times, the chain is driven purely by transnational diffusive motion of the center of mass.

We fix the length of Rouse chain to $N = 1000$ to understand different scaling regimes of monomer MSD with respect

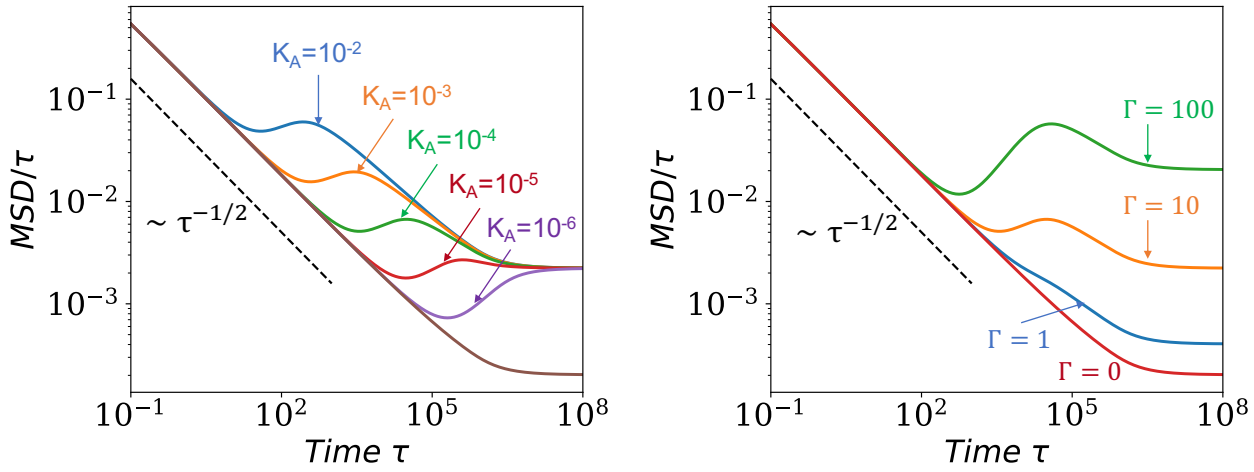

FIG. S4: Mid-point monomer MSD rescaled by time as a function of time for chain length $N = 1000$ are plotted for a fixed $\Gamma = 10$ to show variation of K_A (left) and for a fixed $K_A = 10^{-4}$ to show variation of Γ (right). In both the cases purely thermal results are included (*i.e.* $\Gamma = 0$).

to the mid monomer. In Fig.S4 the mean-square displacement scaled by time is plotted as a function of time; where Γ and K_A are kept fixed in the left and right panel plots respectively. For all values of K_A at timescales $\tau \lesssim K_A^{-1}$, we find the normal sub-diffusive Rouse behavior ($\text{MSD}(\tau) \sim \tau^{0.50}$) that switches to a Γ and K_A dependent super-diffusive regime ($\text{MSD}(\tau) \sim \tau^{1+\epsilon}; \epsilon > 0$) before eventually settling to a plateau that denotes normal diffusion ($\text{MSD}(\tau) \sim \tau^1$) at a higher effective temperature of polymers, given by the rate (K_A) independent factor $(1+\Gamma)T$ as defined earlier. Per biological fluctuations inside of a cellular media for chromosomal motion, this relates to 'agitated' dynamics of individual polymers that 'turns on' per the correlation timescale of biological fluctuations and eventually reaches a steady state diffusive behavior that retains the memory of biological fluctuations even at long enough times.

Similar results to the rescaled MSD or local MSD exponent defined from

$$\alpha(\tau) = \frac{\partial\{\ln(\text{MSD}(\tau))\}}{\partial\{\ln(\tau)\}} \tag{S26}$$

are discussed in ref. [3] and results indicate a combination of thermal and active fluctuations qualitatively define a higher effective temperature and transition from normal sub-diffusive to diffusive behavior through a superdiffusive regime at intermediate times [3].

V. STRUCTURE FACTOR

Static structure factor is defined as,

$$S(\vec{k}) = \frac{1}{N^2}\int_0^N dn_1 \int_0^N dn_2 \Big\langle \exp\Big[i\vec{k}.(\vec{r}(n_1) - \vec{r}(n_2))\Big]\Big\rangle \tag{S27}$$

Evaluating the average over a Gaussian distribution and expressing monomer positions in terms of normal coordinates, we arrive at,

$$S(\vec{k}) = \frac{1}{N^2}\int_0^N dn_1 \int_0^N dn_2 \exp\Big[-\frac{k^2}{6}\Phi_{n_1 n_2}\Big] \tag{S28}$$

where,

$$\Phi_{n_1n_2} = 2\sum_{p=1}^{\infty}\left[\phi_p(n_1) - \phi_p(n_2)\right]^2\langle\vec{X}_p(0)^2\rangle. \tag{S29}$$

and modes ($\phi_p(n)$) are defined in the main text. Simplifying through algebra, the final expression for $\Phi_{n_1n_2}$ is found to be

$$\Phi_{n_1n_2} = \frac{(1+\Gamma)b^2}{3}|n_1-n_2| - \frac{\Gamma b^2}{6\pi K_A^{1/2}}\left[2\sinh\left(\pi K_A^{1/2}|n_1-n_2|\right) - \left(e^{\pi K_A^{1/2}(n_1+n_2)}-1\right)\left(e^{-\pi K_A^{1/2}n_1} - e^{-\pi K_A^{1/2}n_2}\right)^2\right] \tag{S30}$$

For a Rouse model in absence of active fluctuations the above equation reduces to [2], $\Phi_{n_1n_2} = \frac{b^2}{3}|n_1 - n_2|$. While for a purely thermal polymer, one can analytically evaluate the double integral in the static structure factor to give Debye function [2], the above equation must be integrated numerically in order to solve in presence of active forces.

For dynamic structure factor $S(\vec{k};t)$ as defined in the main text, one proceeds the same way by evaluating the average over a Gaussian followed by expansion of monomer motion in terms of mode dynamics. We end up with the crucial quantity $\Phi_{n_1n_2}(t)$, now time dependent and, given by,

$$\Phi_{n_1n_2}(t) = \mathrm{MSD}_{\mathrm{com}}(t) + 2\sum_{p=1}^{\infty}\left[\left(\phi_p(n_1)^2 + \phi_p(n_2)^2\right)\langle\vec{X}_p(0)^2\rangle - \phi_p(n_1)\phi_p(n_2)\langle\vec{X}_p(t)\cdot\vec{X}_p(0)\rangle\right] \tag{S31}$$

To note, dynamic structure factor, $S(\vec{k},t)$ reduces to static structure for $t = 0$. Also, center-of-mass motion is a purely dynamic quantity and does not contribute to static correlations in Fourier space.

VI. FLOW STRUCTURE FACTOR

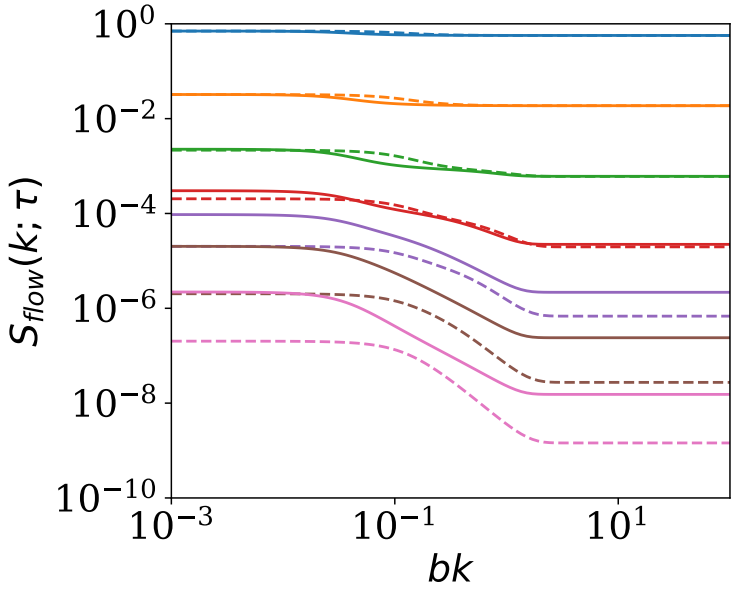

FIG. S5: Flow structure factor as a function of wavevector for time, $\tau = 10^x$ where $x = 0, 1, 2, 3, 4, 5, 6$ (top to bottom) for $N = 1000$, $\Gamma = 10$ and $K_A = 10^{-4}$. Solid and dashed lines are results for active Rouse and thermal Rouse polymer respectively.

To understand mean velocity autocorrelation of chromatin dynamics using displacement correlation spectroscopy

(DCS), ref.[4] defines a flow structure factor where mean flow velocity [4, 5] in Fourier space is given as,

$$F(\vec{k};t)=\sum_{n=1}^{N}\frac{\vec{r}_n(t)-\vec{r}_n(0)}{t}e^{i\vec{k}\cdot\vec{r}_n(0)}\rightarrow\frac{1}{t}\int_0^N dn(\vec{r}_n(t)-\vec{r}_n(0))e^{i\vec{k}\cdot\vec{r}_n(0)} \tag{S32}$$

where we have taken a discrete to continuous transformation. This defines the flow structure factor in Fourier space as,

$$S_{\rm flow}(\vec{k};t)=\frac{1}{Nt^2}\int_0^N dn_1\int_0^N dn_2\big\langle(\vec{r}_{n_1}(t)-\vec{r}_{n_2}(0))\cdot(\vec{r}_{n_1}(t)-\vec{r}_{n_2}(0))e^{i\vec{k}\cdot(\vec{r}_{n_1}(0)-\vec{r}_{n_2}(0))}\big\rangle \tag{S33}$$

While the flow structure factor is a dynamic quantity and relates with the dynamic structure factor (that calculates density correlation in Fourier space), expressing flow structure in terms of known quantities requires us to define a generator function as

$$g(\vec{k};t)=\frac{1}{Nt^2}\int_0^N dn_1\int_0^N dn_2\langle e^{i\vec{k}\cdot(\vec{r}_{n_1}(0)-\vec{r}_{n_2}(0))+\alpha_1(\vec{r}_{n_1}(t)-\vec{r}_{n_1}(0))+\alpha_2(\vec{r}_{n_2}(t)-\vec{r}_{n_2}(0))}\rangle \tag{S34}$$

From the generator function we can note,

$$S_{\rm flow}(\vec{k};t)=\frac{\partial^2 g(\vec{k},t)}{\partial\alpha_1\partial\alpha_2}\Big|_{\{\alpha_1=0,\alpha_2=0\}} \tag{S35}$$

Performing the Gaussian average over the generator function followed by a mode expansion and calculating partial derivatives, we find,

$$S_{\rm flow}(\vec{k};t)=\frac{1}{Nt^2}\int_0^N dn_1\int_0^N dn_2\Big\{\Big[\sum_{p=0}^{\infty}{\rm MSD}_p(t)\phi_p(n_1)\phi_p(n_2)\Big]\exp\Big(-\frac{1}{2}k^2\sum_{p=1}^{\infty}C_p(0)(\phi_p(n_1)-\phi_p(n_2))^2\Big)\Big\} \tag{S36}$$

Results with growing timescales (from $\tau=1$ to $\tau=10^6$) are indicated in Fig.S5 for both in presence (solid lines) and absence (dashed lines) of active forces. DCS tracking experiments [4] on both wild type (active forces present) and ATP-depleted (no active forces) HeLa cells show at small wavevectors flow structure factor has higher intensity for wild type cells. The observation agrees qualitatively with our theoretical analysis as shown in Fig.S5. At long wavevectors experiments conclude a higher effective noise temperature than the actual temperature of the system in presence of active forces from higher flow structure factor intensity in the high k limit. This agrees with our results too since solid line plateau always lies above plateau intensity of pure thermal polymer. This strong qualitative connection with experimental results indicate the importance of active forces in understanding chromatin dynamics.

VII. WILEMSKI-FIXMAN LOOP FORMATION TIMESCALE

Two correlated theories exist to describe the spontaneous loop formation of a polymer chain, by Wilemski and Fixman (WF)[6, 7] and by Szabo, Schulten, and Schulten (SSS)[8]. SSS description suggests probability of contact as a diffusion process in presence of a potential that is dependent on the end-to-end distance of the polymer[8] while WF approach describes looping as a diffusion process in presence of a sink term[6] that ensures loop formation when chain ends are within a 'reaction radius'. We apply the same basic form of WF theory to look at looping timescale for an active-Brownian polymer. The conceptual basis of WF approach relies on stating when the two ends of a polymer come close to each other, a loop would always form. A sink function of arbitrary strength that depends on the end-to-end distance ensures loop formation whenever two ends are close to each other or within the so called 'reaction radius' for looping. Within this context, loop formation time of two polymer ends is given by,

$$\tau_{\circlearrowleft}=\int_0^{\infty}d\tau\Big(\frac{C_{ss}(\tau)}{C_{ss}(\tau\rightarrow\infty)}-1\Big) \tag{S37}$$

where, $C_{ss}(\tau)$ is the sink-sink correlation function,

$$C_{ss}(\tau) = \int d\vec{r} \int d\vec{r}_0 S(r) G(\vec{r}, \tau | \vec{r}_0, 0) S(r_0) \psi_{\rm eq}(r_0) \tag{S38}$$

where $\psi_{\rm eq}(r_0)$ is the equilibrium (steady state for non-equilibrium active Brownian polymer) distribution of the end-to-end distance and $G(\vec{r}, \tau | \vec{r}_0, 0)$ is the conditional probability or Green's function that a chain with end-to-end distance $\vec{r}_0$ at time $\tau = 0$ has the end-to-end distance $\vec{r}$ at time τ. For an active-Brownian polymer considered here, we note that $\psi_{\rm eq}(r_0)$ represents the steady-state distribution of the active polymer. As such, the active forces tend to swell the polymer, which is reflected in the initial condition of the polymer chain. For the looping dynamics, we focus on timescales beyond the active-force decorrelation time, since the looping dynamics coincide with long time-scale processes at the largest distance along the polymer chain. In essence $C_{ss}(\tau)$ describes the probability that the polymer exists in the looped state at time τ given it starts with a looped state at time $\tau = 0$. As stated before, the sink function $S(r)$ provides the idea of 'capture size' or average separation that causes two points to form a loop. Since individual normal modes are Gaussian and end-to-end distance is a linear combination of normal modes, we find the Green's function is still a Gaussian, and is given by

$$G(\vec{r}, \tau | \vec{r}_0, 0) = \Big[\frac{3}{2\pi \langle r_{eA}^2 \rangle (1 - \phi_A^2(\tau))}\Big]^{3/2} \exp\Big[- \frac{3}{2\pi \langle r_{eA}^2 \rangle} \frac{(\vec{r} - \phi_A(\tau)\vec{r}_0)^2}{(1 - \phi_A^2(\tau))}\Big], \tag{S39}$$

where $\phi_A(\tau)$ is the normalized mean-square end-to-end vector correlation, found to be

$$\begin{aligned} \phi_A(\tau) = \frac{\langle \vec{r}(\tau) \cdot \vec{r}(0) \rangle}{\langle r_{eA}^2 \rangle} &= \frac{8/\pi^2}{1 + \Gamma\Big[1 - \frac{2}{\pi N \sqrt{K_A}} \tanh\big(\frac{\pi N \sqrt{K_A}}{2}\big)\Big]} \\ &\times \sum_{p=0}^{\infty} \frac{1}{(2p+1)^2} \Big\{ e^{-(2p+1)^2 \tau / N^2} + \frac{\Gamma}{1 - (2p+1)^4/(N^4 K_A^2)} \Big[e^{-(2p+1)^2 \tau / N^2} - \frac{(2p+1)^2}{N^2 K_A} e^{-K_A \tau} \Big] \Big\} \end{aligned} \tag{S40}$$

which has the time and active force dependent contributions on top of Brownian-only polymer. To illustrate the dynamics of the end-to-end distance of the chain we plot the Green's function given in Eq. S39 for both Rouse and active-Rouse model for a chain length of $N = 100$, $\Gamma = 10$ and $K_A = 10^{-4}$ in Fig. S6. For all timescales and initial values of parameter space (spanning chain length N, strength of active force Γ and active rate K_A) we find $G[\vec{r}, \tau | \vec{r}_0, 0]$ always peaks at $\vec{r} = \vec{r}_0$. Comparing Rouse and active-Rouse model we note the Green's function differ only at longer time where the Green's function for active-Rouse model has larger 'width'. Conceptually this means presence of active forces increases the probability of fluctuation of end-to-end distance around $\vec{r}_0$.

Performing the angular average in Eq. S38 we find,

$$C_{ss}(\tau) = \Big(\frac{3}{2\pi \langle r_{eA}^2 \rangle}\Big)^3 \frac{1}{[1 - \phi_A^2(\tau)]^{3/2}} \int_0^{\infty} 4\pi r^2 S(r) dr \int_0^{\infty} 4\pi r_0^2 S(r_0) dr_0 \exp\Big(- \frac{3}{2\langle r_{eA}^2 \rangle} \frac{r^2 + r_0^2}{1 - \phi_A^2(\tau)}\Big) \frac{\sinh\left[\alpha(\tau, r, r_0)\right]}{\alpha(\tau, r, r_0)} \tag{S41}$$

where,

$$\alpha(\tau, r, r_0) = \frac{3 \phi_A(\tau) r r_0}{\langle r_{eA}^2 \rangle (1 - \phi_A^2(\tau))} \tag{S42}$$

This completes the extension of WF approach to understand looping timescale for an active-Brownian polymer. To further make progress we must assert a suitable function for the sink, which for our purpose is taken as the radial delta function $S(r) = \delta(r - a)$ [9]. Here a is termed as the 'capture radius' and the choice of delta function sink simplifies the results significantly, leading to,

$$\frac{C_{ss}(\tau)}{C_{ss}(\tau \to \infty)} = \frac{\exp\Big(- \frac{2 x_0 \phi_A^2(\tau)}{1 - \phi_A^2(\tau)}\Big) \sinh\Big(\frac{2 x_0 \phi_A(\tau)}{1 - \phi_A^2(\tau)}\Big)}{2 x_0 \phi_A(\tau) \sqrt{1 - \phi_A^2(\tau)}} \tag{S43}$$

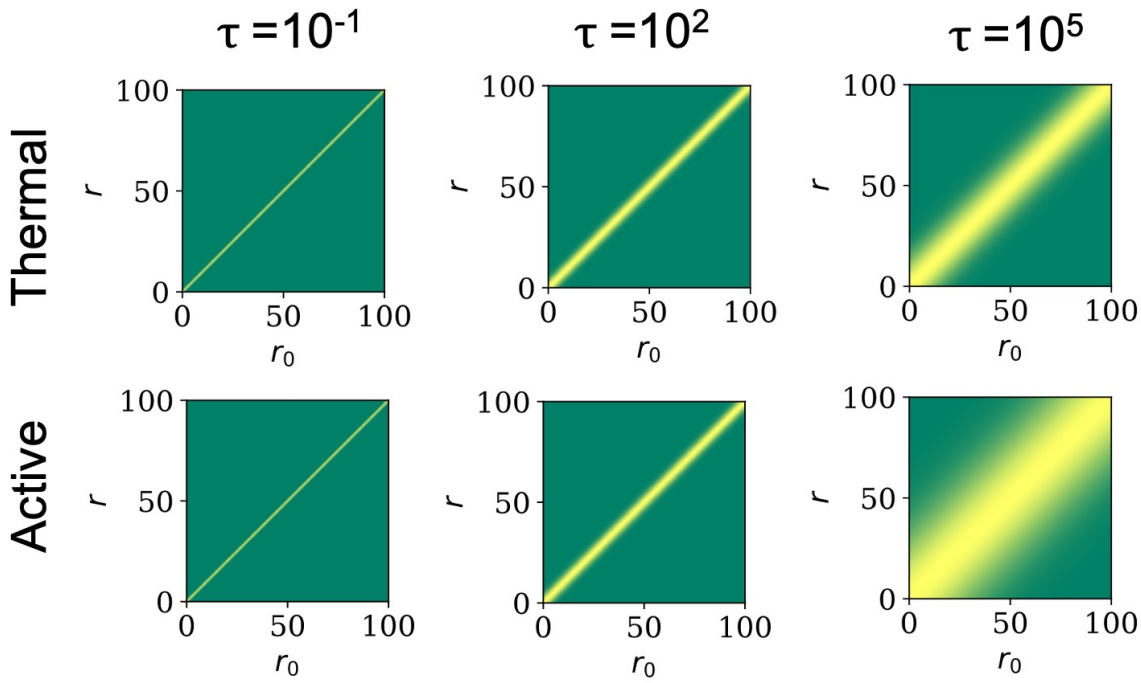

FIG. S6: Amplitude of Green's function for the end-to-end vector distance for different times for both Brownian-only and Active-Brownian polymer with $N = 100$, $\Gamma = 10$, $K_A = 10^{-4}$.

where, $x_0 = \frac{3a^2}{2\langle r_{eA}^2\rangle}$. Hence, the final expression for loop formation time is given by,

$$\tau_{\circlearrowleft}^{A} = \int_0^\infty d\tau \left[\frac{\exp\left(-\frac{2x_0\phi_A^2(\tau)}{1-\phi_A^2(\tau)}\right)\sinh\left(\frac{2x_0\phi_A(\tau)}{1-\phi_A^2(\tau)}\right)}{2x_0\phi_A(\tau)\sqrt{1-\phi_A^2(\tau)}} - 1 \right] \tag{S44}$$

For a pure Rouse polymer the results reduce to,

$$\tau_{\circlearrowleft}^{B} = \int_0^\infty dt \left[\frac{\exp\left(-\frac{2x_0\phi_B^2(t)}{1-\phi_B^2(t)}\right)\sinh\left(\frac{2x_0\phi_B(t)}{1-\phi_B^2(t)}\right)}{2x_0\phi_B(t)\sqrt{1-\phi_B^2(t)}} - 1 \right] \tag{S45}$$

with a modified, $x_0 = \frac{3a^2}{2\langle r_{eB}^2\rangle}$ and normalized mean-square end-to-end vector correlation for Brownian-only polymer is found from asserting $\Gamma = 0$ in Eq. S40,

$$\phi_B(\tau) = \frac{\langle \vec{r}(\tau)\cdot\vec{r}(0)\rangle}{\langle r_{eB}^2\rangle} = \frac{8}{\pi^2}\sum_{p=0}^{\infty}\frac{e^{-(2p+1)^2\tau/N^2}}{(2p+1)^2} \tag{S46}$$

Fig.S7 plots the normalized end-to-end distance time correlation function as defined in Eq. S40 and Eq. S46 for a fixed $N = 100$ and $\Gamma = 10$ for several active rates. The curve in black dashed line corresponds to thermal Rouse polymer and indicates only Brownian channel of relaxation. In both the limits of $N^2K_A \ll 1$ (orange) and $N^2K_A \gg 1$ (blue) correlation decay is primary dominated by the Brownian force channel while in the $N^2K_A \sim 1$ regime, we notice significant changes in how correlation function is altered. The impact of this on the looping timescale is further explored later.

It should be noted that for the delta function sink, $C(\tau)$ has a singularity at $\tau = 0$ and prevents an intuitive probabilistic interpretation of the argument inside Eq. S44 or Eq. S45 [10]. For numerical integration to calculate the

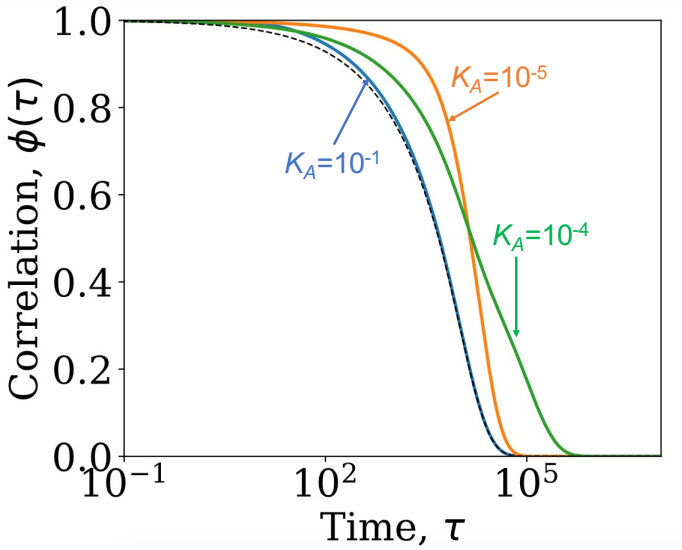

FIG. S7: Normalized end-to-end vector correlation for a chain of length $N = 100$ with active force $\Gamma = 10$ for a range of K_A values. Brownian-only result is indicated in black dashed line.

loop formation time, we can approximate the integrand for both active and thermal cases to

$$\frac{\exp\left(-\frac{2x_0\phi^2(\tau)}{1-\phi^2(\tau)}\right)\sinh\left(\frac{2x_0\phi(\tau)}{1-\phi^2(\tau)}\right)}{2x_0\phi(\tau)\sqrt{1-\phi^2(\tau)}} \approx \frac{1}{(1-\phi^2)^{3/2}} - \frac{2\phi^2}{(1-\phi^2)^{5/2}}x_0 + \frac{2\phi^2(1+3\phi^2)}{3(1-\phi^2)^{7/2}}x_0^2 + ... \tag{S47}$$

If only the 0^{th} order term in x_0 is kept in the above expansion, the results reduce to that of a different choice of sink function, namely the Heaviside sink [9] and we find,

$$\tau_{\circlearrowleft} \approx \int_0^\infty d\tau\Big[\frac{1}{(1-\phi^2(\tau))^{3/2}} - 1\Big] \tag{S48}$$

The above equation is exact if we conceptualize loop formation as zero distance between the two end points of a polymer chain, since, in such cases $X_0 \to 0$ should be considered in Eq. S47. One motivation to look at such limit is the applicability of WF approach with delta sink in correctly identifying the loop formation timescale for a Brownian polymer as discussed in ref. [10].

Before proceeding further, we consider two limits of N^2K_A to understand why looping timescale in presence of active forces only impacts intermediate N and the time is approximately same for either of very small or very large N.

Large-N limit: To understand the large N limit, we consider $N^2K_A \to \infty$ in Eq. S40 to find

$$\lim_{N^2K_A\to\infty}\phi_A(\tau) \to \frac{8}{\pi^2(1+\Gamma)}\sum_{p=0}^{\infty}\frac{1}{(2p+1)^2}\Big[e^{-(2p+1)^2\tau/N^2} + \Gamma e^{-(2p+1)^2\tau/N^2}\Big] = \phi_B(\tau) \tag{S49}$$

In other words, the normalized end-to-end correlation of active Brownian polymer is essentially same as that of a Brownian only polymer. A physical interpretation of this can be given by thinking about the critical lengthscale associated with active force de-correlation is much smaller than chain scale relaxation, hence chain relaxation is oblivious to the presence of active forces in the limit of $N \gg 1/\sqrt{K_A}$. Hence we should expect the loop formation timescale for very large N^2K_A should be similar to that of a Brownian-only polymer.

Small N limit: Understanding the small N limit is slightly more complicated than the large N behavior. If we consider $N^2K_A \to 0$ in Eq. S40 to again find, $\lim_{N^2K_A\to 0}\phi_A(\tau) \to \phi_B(\tau)$, however for small N, the first order contribution to $\phi_A(\tau)$ also matters, resulting in a non-universal N dependence. A physical interpretation is the timescale to relax active forces is beyond the chain relaxation .

Analyzing the two limits we see only in the intermediate timescales where active force correlation time competes with chain-scale relaxation, we can expect looping timescale to predict changes with respect to the background Brownian only polymer.

VIII. RECONFIGURATION TIMESCALE

Reconfiguration time of a polymer provides an idea about the characteristic decay time of the correlation of any two points on a chain and primarily used to characterize protein dynamics where two points of a protein can be fluorescent probed and dynamical evolution of the chain can be studied using resonance energy transfer methods. Formally the reconfiguration time for end-to-end vector is defined as,

$$\tau_{\rm r} = \int_0^\infty \phi(\tau) d\tau \tag{S50}$$

where $\phi(\tau)$ is the normalized end-to-end vector correlation function. We consider two cases of reconfiguration time below, where active forces are absent or present.

Case I, no active forces: In absence of any active forces, normalized end-to-end vector correlation function is given as,

$$\phi_B(\tau) = \frac{8}{\pi^2} \sum_{p=0}^{\infty} \frac{e^{-(2p+1)^2\tau/N^2}}{(2p+1)^2} \tag{S51}$$

Hence, the reconfiguration time for the pure Rouse dynamics is given by,

$$\begin{aligned} \tau_{\rm r}^B &= \frac{8}{\pi^2} \sum_{p=0}^{\infty} \frac{1}{(2p+1)^2} \int_0^\infty e^{-(2p+1)^2\tau/N^2} d\tau \\ &= \frac{8N^2}{\pi^2} \sum_{p=0}^{\infty} \frac{1}{(2p+1)^4} = \frac{\pi^2}{12} N^2 \end{aligned} \tag{S52}$$

The last equality uses the exact relation, $\sum_{p=0}^{\infty} \frac{1}{(2p+1)^4} = \frac{\pi^4}{96}$. Hence we can easily note that, $\tau_{\rm conf.}^B \sim N^2$ for any arbitrary value of N.

Case II, active forces: When active forces are non-zero we can once again write the end-to-end vector correlation as a function of swelling ratio α, and the strength and timescale of active drive, and given as

$$\phi_A(\tau) = \frac{8}{\alpha\pi^2} \sum_{p=0}^{\infty} \frac{1}{(2p+1)^2} \Big\{ e^{-(2p+1)^2\tau/N^2} + \frac{\Gamma}{1-(2p+1)^4/(N^4K_A^2)} \Big[e^{-(2p+1)^2\tau/N^2} - \frac{(2p+1)^2}{N^2K_A} e^{-K_A\tau} \Big] \Big\} \tag{S53}$$

where,

$$\alpha = \left[1 + \Gamma \Big\{ 1 - \frac{2}{\pi N\sqrt{K_A}} \tanh\big(\frac{\pi N\sqrt{K_A}}{2}\big) \Big\} \right] \tag{S54}$$

The summation and the integral can be evaluated analytically and found to be,

$$\tau_{\rm r}^A = \int_0^\infty \phi_A(\tau) d\tau = \frac{\pi^2}{12} \frac{1+\Gamma}{\alpha} N^2 \tag{S55}$$

where, $1 \leq \frac{1+\Gamma}{\alpha}$, and the fraction is a function of N, hence, the size dependence in not precisely N^2 for Rouse dynamics with active forces.

We plot the reconfiguration time Fig.S8. Reconfiguration times are found to be fully analytic and chain-length dependence can be easily analyzed. Rouse chain follows typical N^2 dependence as shown in blue in Fig.S8. Active-Rouse chain does not follow the same power law for all lengthscales due to the N-dependent factor $(1+\Gamma)/\alpha(N)$. In

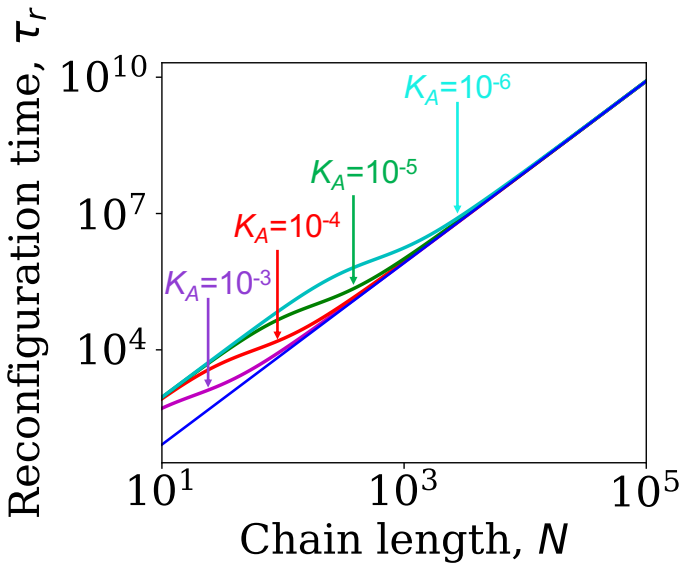

FIG. S8: Reconfiguration time as a function of chain length, for $\Gamma = 0$ (no active forces, blue) and $\Gamma = 10$ (others) for a range of K_A values.

the limit of $N^2 K_A \ll 1$, swelling ratio, $\alpha(N) \to 1$ and the reconfiguration time follows a $\tau_r^A \sim N^2$ power law, albeit with a higher amplitude. In the limit $N^2 K_A \gg 1$, we find the swelling ratio reaches its maximum, $\alpha(N) \to 1 + \Gamma$ and we see, $\tau_r^A \sim N^2$ with the same pre-factor as that of a thermal Rouse chain. Hence all the active-Rouse results merge to the blue curve at sufficiently high values of chain length N. Similar results for chain reconfiguration dynamics have been found showing reconfiguration dynamics is largely controlled by the rate of active force relaxation rather than the magnitude of active force [11].

[1] A. Ghosh and A. J. Spakowitz, Physical Review E (2022).
[2] M. Doi, S. F. Edwards, and S. F. Edwards, *The theory of polymer dynamics*, Vol. 73 (Oxford University Press, 1988).
[3] D. Osmanović and Y. Rabin, Soft Matter **13**, 963 (2017).
[4] R. Bruinsma, A. Y. Grosberg, Y. Rabin, and A. Zidovska, Biophysical journal **106**, 1871 (2014).
[5] A. Zidovska, D. A. Weitz, and T. J. Mitchison, Proceedings of the National Academy of Sciences **110**, 15555 (2013).
[6] G. Wilemski and M. Fixman, The Journal of Chemical Physics **60**, 866 (1974).
[7] G. Wilemski and M. Fixman, The Journal of Chemical Physics **60**, 878 (1974).
[8] A. Szabo, K. Schulten, and Z. Schulten, The Journal of Chemical Physics **72**, 4350 (1980).
[9] R. W. Pastor, R. Zwanzig, and A. Szabo, The Journal of Chemical Physics **105**, 3878 (1996).
[10] F. X.-F. Ye, P. Stinis, and H. Qian, SIAM Journal on Applied Mathematics **78**, 104 (2018).
[11] N. Samanta and R. Chakrabarti, Journal of Physics A: Mathematical and Theoretical **49**, 195601 (2016).